Available online at www.sciencedirect.com

ScienceDirect

www.elsevier.com/locate/jes

JES JOURNAL OF ENVIRONMENTAL SCIENCES

www.jesc.ac.cn

Understanding unusually high levels of peroxyacetyl nitrate (PAN) in winter in Urban Jinan, China

Lu Liu[1], *Xinfeng Wang*[1], *Jianmin Chen*[1,2,3,*], *Likun Xue*[1,3], *Wenxing Wang*[1], *Liang Wen*[1], *Dandan Li*[1], *Tianshu Chen*[1]

1. *Environment Research Institute, School of Environmental Science and Engineering, Shandong University, Ji'nan 250100, China*
2. *Shanghai Key Laboratory of Atmospheric Particle Pollution and Prevention, Department of Environmental Science and Engineering, Institute of Atmospheric Sciences, Fudan University, Shanghai 200433, China*
3. *Institute for Climate and Global Change Research, School of Atmospheric Sciences, Nanjing University, Nanjing 210008, China*

ARTICLE INFO

Article history:
Received 21 December 2017
Revised 15 May 2018
Accepted 16 May 2018
Available online 24 May 2018

Keywords:
Peroxyacetyl nitrate
Winter
Haze episodes
North China Plain

ABSTRACT

Peroxyacetyl nitrate (PAN), as a major secondary pollutant, has gained increasing worldwide attentions, but relevant studies in China are still quite limited. During winter of 2015 to summer of 2016, the ambient levels of PAN were measured continuously by an automatic gas chromatograph equipped with an electron capture detector (GC–ECD) analyzer at an urban site in Jinan (China), with related parameters including concentrations of O_3, NO, NO_2, $PM_{2.5}$, HONO, the photolysis rate constant of NO_2 and meteorological factors observed concurrently. The mean and maximum values of PAN concentration were (1.89 ± 1.42) and 9.61 ppbv respectively in winter, and (2.54 ± 1.44) and 13.47 ppbv respectively in summer. Unusually high levels of PAN were observed during severe haze episodes in winter, and the formation mechanisms of them were emphatically discussed. Study showed that high levels of PAN in winter were mainly caused by local accumulation and strong photochemical reactions during haze episodes, while mass transport played only a minor role. Accelerated photochemical reactions (compared to winter days without haze) during haze episodes were deduced by the higher concentrations but shorter lifetimes of PAN, which was further supported by the sufficient solar radiation in the photolysis band along with the high concentrations of precursors (NO_2, VOCs) and HONO during haze episodes. In addition, significant PAN accumulation during calm weather of haze episodes was verified by meteorological data.

Introduction

Peroxyacetyl nitrate (PAN), a typical secondary pollutant, is formed by photochemical reactions of volatile organic compounds (VOCs) and nitrogen oxides (NO_x) in the atmosphere (Aikin et al., 1982). PAN is often considered as a marker of photochemical pollution due to its exclusive secondary origin, and it is a harmful substance for human health and vegetation (Peak and Belser, 1969). Because of its low solubility in water and thermal instability, thermal decomposition is the main sink mechanism of PAN compared to wet deposition and photolysis (Gaffney et al., 1993). Because of its long lifetime at low temperature, PAN can be transported over long distances in the upper troposphere from polluted regions, and

* *Corresponding author. E-mail:* jmchen@sdu.edu.cn (Jianmin Chen).

https://doi.org/10.1016/j.jes.2018.05.015
1001-0742/

it could release NO_x in some remote areas through thermal decomposition (Beine et al., 1997; Kenley and Hendry, 1982). Thus, PAN is considered as a temporary NO_x reservoir that may affect the NO_x level and consequently O_3 production in remote areas.

PAN was first detected in the photochemical smog events of Los Angeles in the 1950s (Stephens et al., 1956) and has been extensively measured around the globe since then. Field measurements showed that the mixing ratios of atmospheric PAN range from a few pptv (in remote areas) (Bottenheim and Gallant, 1989; Moore and Remedios, 2010) to over 40 ppbv (in fragmented metropolitan regions) (Grosjean, 1983, 2003). These values are usually one order of magnitude lower than those of O_3, but the overall bio-toxic effect of PAN is always one or two orders of magnitude greater than that of O_3 (Zhang et al., 2015). In China, photochemical pollution has become a severe environmental issue in recent years due to rapid economic development. However, available data of atmospheric PAN were scarce in China, except in a few regions (Pearl River Delta, Beijing, Lanzhou) (Liu et al., 2010; Wang et al., 2010; Zhang et al., 2009), while researches on O_3 and VOCs were fairly extensive (Shao et al., 2009; Wang et al., 2003; Xu et al., 2008). In addition, previous studies of PAN had been conducted mainly during summer rather than winter, because PAN had obvious diurnal variation and high concentrations during summer. In comparison, wintertime researches were much harder because the high-occurrence of serious pollution events might entail more complex formation and sink mechanisms of gas pollutants.

In this study, the ambient concentrations of PAN were measured from November 2015 to July 2016 in Jinan, China, and this was the first measurement of PAN in the urban area of Shandong Province. We primarily analyzed the mechanism of the unusually high concentrations of PAN in winter (especially during haze episodes) combined with the concurrent data of CCl_4, O_3, NO, NO_2, $PM_{2.5}$, HONO, photolysis rate constant and local meteorological information. Additionally, backward trajectory analysis was used to determine the long-range transport of PAN. Comprehensive analysis of PAN behavior in this study helped to explain the formation and sink mechanisms of PAN, especially in winter.

1. Experiment and methodologies

1.1. Site description

Field measurements were carried out continuously in Jinan (N36°40′, E117°03′), 400 km south of Beijing, from Nov. 2015 to Jul. 2016 (except for a data-deficient gap from Feb. to Mar. in 2016). The population of Jinan is seven million with an urban population of nearly five million. In general, Jinan has a plain topography, but the elevation is higher on the south side than on the north side, and there are small hills on the east and west sides. Thus, the entire area forms a half basin. Due to rapid urbanization, Jinan has faced many air quality problems recently, especially haze and smog (Cui et al., 2016; Gao et al., 2011; Yang et al., 2007). In this study, the monitoring site was located at the Atmospheric Environment Observation Station of Shandong University, on the rooftop of a seven-story building (at a height of approximately 25 m above ground level), and all the gas data (such as NO_x, O_3) were measured at the same location. The monitoring site was surrounded by several residential areas, commercial strips and schools, without large-scale industrial sites or construction projects.

1.2. Measurement techniques

The technique used a gas chromatograph equipped with an electron capture detector (GC–ECD) to simultaneously measure ambient concentrations of PAN, peroxypropionyl nitrate (PPN), and carbon tetrachloride (CCl_4). The detailed introduction of this instrument had been given in many published papers (Zhang et al., 2012, 2015), thus we only briefly mentioned the basic principles of PAN measurement and calibration in this paper. Ambient air was sampled through a Teflon tube (3 mm outside diameter (OD), 6 m length) at a flow rate of 1.5 L/min by a built-in pump (NMP830KNDC, KNF Inc.). Each sampling lasted for 20 sec, and the air sample was temporarily stored in a 0.5-mL GC loop. Then, the pump was switched off for 5 sec to allow the pressure to equilibrate. After that, gas path was switched by ten-port to detection mode: carrier gas (Helium) push the gas sample into the GC-ECD, a well-studied instrument with high sensitivity and selectivity of PAN quantification. In addition, PPN and CCl_4 were measured by the ECD detector at the same time. Because the signals of PPN were always below the detection limits, the PPN data were not included in this study. The minimal variation in CCl_4 concentration could reflect the precision of the instrument due to the constant level of CCl_4 in the ambient air. Analysis of each gas sample took 10 min to complete, and 144 sets of data were obtained every day when the instrument worked continuously. To calibrate the instrument, PAN was generated by irradiation (254 nm) of a gaseous mixture of acetone and NO, and the concentration of PAN was deduced by the flow of the standard NO gas due to the excess acetone. The calibration repeated twice per month and the results showed only small variations (approximately 15%) (Zhang et al., 2012). The detection limits of the GC–ECD (estimated as three times the signal to noise ratio) for PAN, PPN and CCl_4 were 22, 36 and 5 pptv, respectively; the overall uncertainties in the GC–ECD were estimated to be ± 13% (IC calibration) and ±15% (NO_x analyzer calibration) (Zhang et al., 2012). There were some modifications from conditions of the previous studies (Zhang and Mu, 2014; Zhang et al., 2014): we changed the carrier gas from nitrogen to high purity helium to ensure the stability of the instrument, and we used acetone solution instead of acetone gas to ensure an excess of acetone.

During the measurement period, a set of supporting parameters including O_3, NO, NO_2, $PM_{2.5}$, HONO, photolysis rate constant and meteorological data, were collected to explain the variations in the concentrations of PAN. O_3 was measured continuously using the ultraviolet absorption technique (Model 49C, USA) (Wang et al., 2012). NO and NO_2 were detected by the chemiluminescence technique (NO, NO_2, NO_x Analyzer, Thermo Environmental Model 42C, USA), and the NO_2 concentration was corrected by subtraction concurrent PAN concentration to reduce the interference of oxidation of nitrogen oxides (NO_2). The mass concentration of $PM_{2.5}$ was obtained by using a Synchronized Hybrid Ambient Real-Time Particulate Monitor (SHARP Monitor Model 5030, Thermo Fisher Scientific, USA) (Wen et al., 2015). The concentration of HONO was measured by a commercial long path

absorption photometer (QUMA, Model LOPAP-03, Germany) (Xu et al., 2015). The photolysis rate constant of NO_2 was detected through a CCD Actinic Flux Spectrometer (Metcon) and $J(NO_2)$ Filter Radiometer (Metcon, 2-pi-JNO_2-Radiomer, Germany) simultaneously. Wind speed and direction and temperature were continuously collected by an automatic meteorological station (MILOS520, Vaisala, Finland).

2. Results and discussion

2.1. Overall statistics and comparison with other studies

Table 1 presents the statistical values of PAN from Nov. 2015 to Jul. 2016 in Jinan, including the maximum, mean and standard derivation. The statistical data of previous studies reported in the past two decades for other sites are also presented in Table 1 for comparison. Due to the large variation of PAN ambient concentration with temperature, the PAN concentration statistics were roughly divided into two categories: winter and summer. The mean and maximum values of PAN concentration were (1.89 ± 1.42) and 9.6 ppbv respectively in winter, (2.54 ± 1.44) and 13.5 ppbv respectively in summer. The overall levels of PAN in Jinan were obviously higher than those in most other polluted cities listed in Table 1, reflecting severe photochemical pollution in Jinan. The remarkably higher PAN levels observed in summer than in winter were consistent with the seasonal features of atmospheric PAN reported by previous studies (Zhang and Mu, 2014). Furthermore, high PAN levels in winter in Jinan (maximum: 9.6 ppbv, mean: (1.89 ± 1.42) ppbv) were well above the expected value. For example, in winter, the levels of PAN in Jinan were approximately three times those in Beijing (maximum: 3.5 ppbv, mean: 0.7 ppbv), while PAN concentrations were comparable between these two cities in summer season.

The PAN value in Mexico City in 1997 (with a maximum of 34 ppbv) was the highest PAN level observed in the past two decades. It had been reported that the maximum PAN concentration in Mexico City had decreased from 34 ppbv in 1997 to 8 ppbv in 2003 due to the effective control of specific VOC emissions, such as butenes (Gaffney et al., 1999; Marley et al., 2007). The successful control strategies that had been put into place in Mexico City, like reduction of olefin content in liquefied petroleum gas (LPG), had some referential significances for pollution controlling elsewhere. PAN concentrations were remarkably low in most rural sites compared to urban sites. This might be because the NO_x (the necessary precursor of PAN) concentrations in remote places are very low as a result of fewer human activities. In addition, low levels of PAN were found at sites almost without human activities (like ocean, polar region) with extremely varied maximum and mean values, such as PAN researches in the Atlantic (maximum 1.088 ppbv, mean 0.005–0.244 ppbv) and in Antarctica (maximum 52.3 pptv, mean 9.2 pptv). The huge difference between maxima and mean value of PAN indicated the influence of air mass transport. Considering the low-temperature stability of PAN, air mass transport probably affected the ambient concentration of PAN in winter in some

Table 1 – Summery of PAN concentrations in urban Jinan and comparison with other sites in urban and rural areas.

Year	Location	Study period	Maximum concentration (ppbv)	Mean concentration (ppbv)	Reference
Urban					
1997	Mexico City	Feb.–Mar.	34		(Gaffney et al., 1999)
1997	Santa Rita, Brazil	21–27 Mar.	6.67	0.40 ± 0.63	Grosjean et al. (2001)
1997	Southern California, USA	Jul.–Oct.	0.72	0.25 ± 0.12	Kean et al. (2001)
2000	Houston, Texas, USA		14		Roberts et al. (2002)
2002	Santiago, Chile	Sep.	3.9	2.8	Rubio et al. (2005)
		Dec.	9.8	5.3	Rubio et al. (2005)
2003	Santiago, Chile	Jan.	22	6.4	Rubio et al. (2005)
2003	Mexico City	Apr.–May	8		Marley et al. (2007)
2004–2005	Korea University, Seoul	May–Jun.	10.4	0.8	Lee et al. (2008)
2006	Lanzhou, China	23 Jun., 17 Jul.	9.13	0.76 ± 0.89	Zhang et al. (2009)
2006	Pearl River Delta, China	Summer	3.9	1.32	Wang et al. (2010)
2010	Beijing, China	25 Jan.–22 Mar.	3.51	0.7 (0.23–3.51)	Zhang et al. (2014)
		Jun.–Sep.	12.5	2.61 ± 2.57	Zhang et al. (2015)
2011	Gwang Jin, Seoul, South Korea	Jan.–Dec.	5.03	0.64	Lee et al. (2013)
2015–2016	Jinan, China	4 Nov.–next 14 Jan.	9.61	1.89 ± 1.42	This study
2016		1 Apr.–19 Jul.	13.47	2.54 ± 1.44	This study
Rural					
1998	Atlantic	30 May–21 Jun.	1.088	0.005–0.244	Jacobi et al. (1999)
2000	Houston, USA	Aug.–Sep.	6.5	0.48	Roberts et al. (2001, 2003)
2003	Jungfraujoch	Feb.–Mar.	1.29	0.14	Whalley et al. (2004)
2004–2005	Brunt Ice Shelf, Antarctica	Jul. 2004–Jan. 2005	52.3 (pptv)	9.2 (pptv)	Mills et al. (2007)
2006	Mt. Waliguan, China	22 Jul.–16 Aug.	1.4	0.44 ± 0.16	Zhang et al. (2009)
2006	Mount Bachelor, USA	Apr.–May	3.074	0.34 ± 0.37	Wolfe et al. (2007)
2006	Yufa, Beijing, China	3–12 Sep.	2.5	0.6	Zhang et al. (2011)
2010	GCO, Jeju Island, Korea	10 Oct.–6 Nov.	2.4	0.6	Han et al. (2017)
2014	Auchencorth Moss, UK	24 Apr.–6 May	1.57	0.46 ± 0.03	Malley et al. (2016)

PAN: peroxyacetyl nitrate.

degree, thus a detailed discussion of PAN transport contribution in this study is given in Section 2.3.

2.2. Time series and characteristics

The time series of PAN from 4 Nov. 2015 to 19 Jul. 2016 are plotted in Fig. 2a. The ambient concentrations of PAN showed high variability and generally reached a peak in the afternoon and then decreased until the next morning in summer (shown in Fig. 3). But during wintertime, ambient PAN concentrations did not show that typical diurnal variation frequently. As shown in Table 1, the PAN concentrations in winter in Jinan were significantly higher than those in other polluted cities of China, such as Beijing. Furthermore, at the same time of winter observation, severe haze episodes appeared and lasted for weeks, which implied a possible connection between haze episodes and unusually high PAN levels. To figure out this connection, the time series of ambient concentrations of PAN, CCl_4 and $PM_{2.5}$ during the period from 18 Dec. 2015 to 14 Jan. 2016 are shown in detail in Fig. 2b.

Two major haze episodes, 19–25 Dec. 2015 and 2–5 Jan. 2016, are clearly shown in Fig. 2b (marked with dashed frame): In Fig. 2b, the concentrations of PAN showed a similar trend as that of $PM_{2.5}$ concentrations, which suggested that unusually high concentrations of PAN in winter might be related to heavy haze episodes. This conjecture had been presented in previous researches (Han et al., 2017; Zhang and Mu, 2014) which also frequently observed unusual PAN enhancements during haze episodes. During these two haze episodes, the $PM_{2.5}$ concentration was continuously above 300 $\mu g/m^3$ and even reached 700 $\mu g/m^3$. These levels of $PM_{2.5}$ were high enough to be classified as severe haze episodes when compared with the 24-hour Chinese National Ambient Air Quality Standard of $PM_{2.5}$ (75 $\mu g/m^3$) (Martini et al., 2015) and the Jinan annual average concentration of $PM_{2.5}$ (149 $\mu g/m^3$) (Yang et al., 2012). The relatively stable CCl_4 concentrations during this month indicated the favorable stability of the instrument (GC–ECD). But there were a few unusual CCl_4 peaks, which might be explained by limited usage as cleaning agent in the manufacturing sector (Zhang and Mu, 2014).

To determine the causes of unusually high levels of PAN in winter, we chose four typical cases for a comparative analysis: case A (2015/12/23), case B (2016/01/03), case C (2016/01/08), and case D (2016/05/31), which represented the maximum PAN peak in winter, the night-time PAN peak in winter, the regular daytime PAN peak in winter and the maximum PAN peak in summer, respectively. More winter cases were chosen in view of complex environmental influence factors of PAN levels in winter in Jinan, like pollution level and meteorological factor. The typical diurnal variations of PAN, O_3, O_x, NO, $PM_{2.5}$ and the wind vector at Jinan in the four cases are given in Fig. 3. Firstly, unlike the summer case (D), the winter cases (A, B, and C) had much higher concentrations of NO_x ($NO + NO_2$) and $PM_{2.5}$, indicating serious pollution in winter (Fujiwara et al., 2014). In addition, the distinctive NO peak at approximately 8 am in the winter cases showed that the mobile source should be one major emission source during winter. The obviously lower wind speeds in winter than in summer illustrated that the meteorological environment during winter could benefit the local accumulation of PAN. After seasonal comparison, we could make a preliminary deduction that lower wind speeds and more serious air pollution in winter might be the potential seasonal factors contributing to the high levels of PAN.

To understand the change of PAN concentration during haze episodes, we compared case A and case C: case C represents the "average" winter diurnal variation without any special pollution episode, and case A represents the maximum PAN peak in a haze episode in winter, with PAN value of 9.6 ppbv. As compared with case C, case A showed significant enhancement of PAN, O_x and O_3 concentrations in the afternoon and the decrease after sunset, which was in accordance with the characteristics of strong photochemical reactions (such as case D). Therefore, one great possibility was there were significant indigenous photochemical sources of PAN during haze episodes. Nevertheless, this conjecture contrasted with the common notion that weak solar irradiation during haze episodes could result in slow photochemical reactions. Thus, more discussions about this deduction are given in Section 2.4.2 for greater accuracy. O_3, a typical photochemical pollutant as well as PAN, frequently showed a consistent trend with PAN and consequently was often used to understand PAN concentration variation. In wintertime, O_3 levels were extremely low, mainly due to intense O_3 titration of NO on the polluted day; thus, we used the value O_x ($O_3 + NO_2$) to approximate the real value of O_3 generation. The enhancement of PAN concentration in Fig. 3b after sunset contrasted with the continuous decrease of O_x and O_3 concentration coupled with fast-changing winds. According to previously reported cases (Zhang et al., 2015), the preliminary explanation of this phenomenon was that the night peak of PAN was caused by long-range transport, which is further proved by a trajectory model in Section 2.3. Based on above discussions, we could speculate that long-range transport, accumulation, and the faster photochemical reactions (compared to wintertime without haze) during haze episodes might be three main factors of the unusually high concentrations of PAN in winter, and further discussions are presented in Sections 2.3 and 2.4 to verify this speculation.

2.3. Long-range transport

PAN could be long-range transported in the upper air due to its low-temperature stability. To determine whether long-range transport was a main cause of the high PAN levels in winter, we draw 72-hr backward trajectory lines calculated by the Hybrid Single Particle Lagrangian Integrated Trajectory Model HYSPLIT (NOAA, http://ready.arl.noaa.gov/HYSPLIT.php) for every day in Fig. 2b, and the transport pathways were color-coded to indicate the corresponding PAN concentration at the end time. The end time was set to 24:00 local time to avoid the photochemical interferences of PAN concentration. As shown in Fig. 4a, only trajectory line 17 on 3 Jan. 2016, corresponding to case B in Fig. 3, showed an obvious air mass transport coupled with high level of PAN at midnight. This trajectory line was a good representation of PAN long-range transport combined with the discussion of case B in Section 2.2. Except for transport, the nighttime high value of PAN also might be related to NO_3-radical-initiated reactions, which is an important source of secondary organic aerosols at night (Mellouki et al., 2015). Other trajectory lines with high PAN concentration illustrated that air mass moved

slowly and hovered around our site, indicating that the high concentrations of PAN were mainly from local sources.

To further confirm the effect of transport, the concurrent scatter plots of wind direction and speed are illustrated in Fig. 4b, where hourly data points were color-coded to show the corresponding PAN concentrations. It was clear that most high PAN concentrations appeared in the east and northeast winds with wind speed lower than 2 m/sec, and this wind speed in winter could favor PAN local accumulation (Zhang et al., 2014). In addition, many emission sources lay to the east and northeast of our site, as shown in Fig. 1, and thus the oxidized exhaust (loaded with various pollutants) from factories might also contribute to the high levels of PAN. In the strong southwest and east winds (>3 m/s), most of observed concentrations of PAN stayed low (<3 ppbv), indicating that wind blow (mostly southwest and east winds) was a primary pathway of PAN removal in winter in Jinan. In summary, long-range transport might contribute to the high PAN concentrations in winter to a certain extent, but in most cases, extremely high concentrations of PAN were locally generated and accumulated.

2.4. Local sources

2.4.1. Lifetimes of PAN

Above discussion had speculated that accumulation and local generation mainly contributed to the high PAN concentrations in winter, and next we used the lifetime of PAN under different situations calculated by reaction kinetics of PAN formation and decomposition reactions (Reactions (R1) through (R4)) to further confirm that deduction. PAN has no natural source and is mainly generated by carbonyls reacting with OH (or photolysis) in the presence of NO_2, as shown in (R1) and (R2). Thermal decomposition (R-2) is determined to be a prominent removal pathway of PAN, and its rate has an obvious change with the ambient temperature.

$$\text{VOCs} + \text{OH or } h\nu \xrightarrow{O_2} CH_3C(O)OO\cdot + \text{products} \quad (R1)$$

$$CH_3C(O)OO\cdot + NO_2 \rightarrow \text{PAN} \quad (R2)$$

$$\text{PAN} \rightarrow CH_3C(O)OO\cdot + NO_2 \quad (R-2)$$

$$CH_3C(O)OO\cdot + NO \rightarrow CH_3\cdot + CO_2 + NO_2 \quad (R3)$$

Based on the above reactions, PAN thermal decomposition rate could be calculated as follows (Zhang et al., 2015, 2011).

$$-\frac{d\ln[\text{PAN}]}{dt} = \frac{k_{-2}k_3[NO]}{k_3[NO] + k_2[NO_2]} \quad (1)$$

If we ignored other sink pathways and considered only thermal decomposition, the rough lifetime of PAN in the atmosphere could be derived from Eq. (2):

$$\tau(\text{PAN}) = \frac{1}{k_{-2}}\left(1 + \frac{k_2[NO_2]}{k_3[NO]}\right) \quad (2)$$

where, τ (PAN) is the atmospheric lifetime of PAN (sec); k_2 is the rate constant for Reaction (R2) (cm^3/(molecule·sec)); k_{-2} is

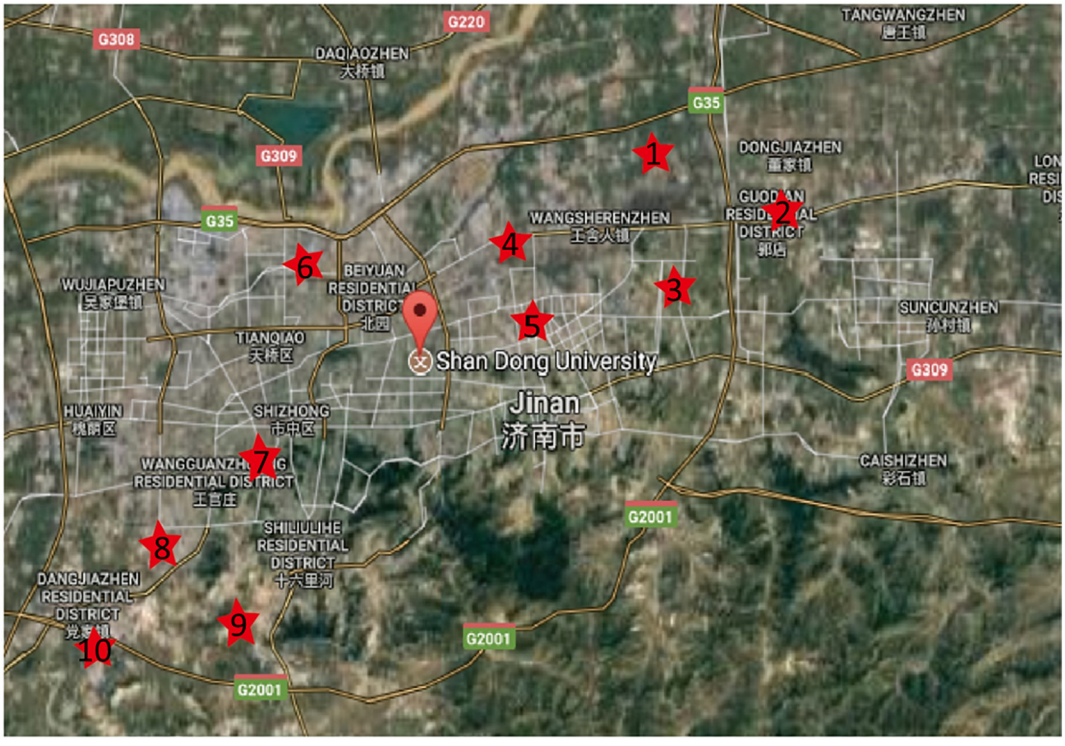

Fig. 1 – Map showing the location and terrain of the observation site in Jinan, China and the main emission sources in the surrounding area. 1: Shandong Steel Plant; 2: Gengchen Steel Plant; 3: Jinan Oil Refinery Plant; 4: Huangtai Thermal Power Plant; 5: Dongxin Power Plant; 6: North Suburban Thermal Power Plant; 7: South Suburban Thermal Power Plant; 8: Shandong Cement Plant; 9: Wohushan Cement Plant; 10: Shijichuangxin Cement Plant.

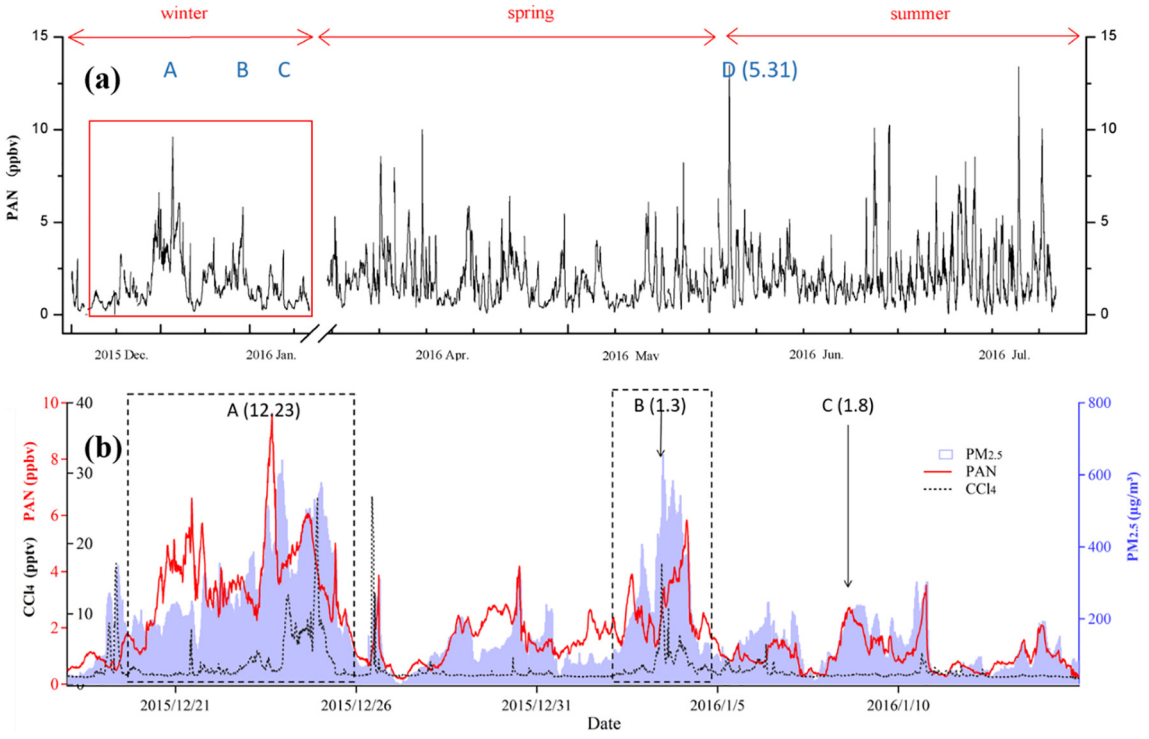

Fig. 2 – Time series of PAN concentration in Jinan. (a) Time series of PAN concentration between 04 Nov. 2015 and 19 Jul. 2016. Four typical cases, labeled a through d, were selected for further analysis; (b) a close-up of the PAN profile in winter during the period from 18 Dec. 2015 to 14 Jan. 2016, combined with the concentrations of CCl_4 and $PM_{2.5}$. The two dashed frames represented two severe long-duration haze events in winter. PAN: peroxyacetyl nitrate.

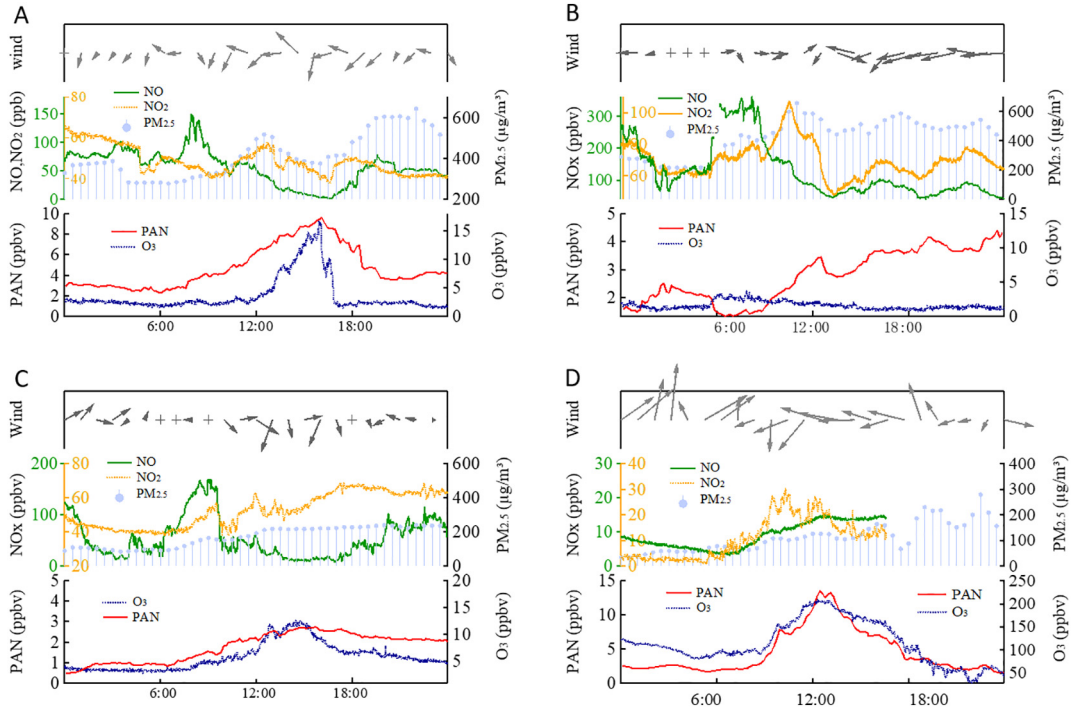

Fig. 3 – Diurnal cycles of PAN, O_3, O_x (NO_2 + O_3), NO, $PM_{2.5}$ and wind vector at Jinan on case A (23 Dec. 2015), case B (3 Jan. 2016), case C (8 Jan. 2016), and case D (31 May 2016). Black arrows represent wind vectors.

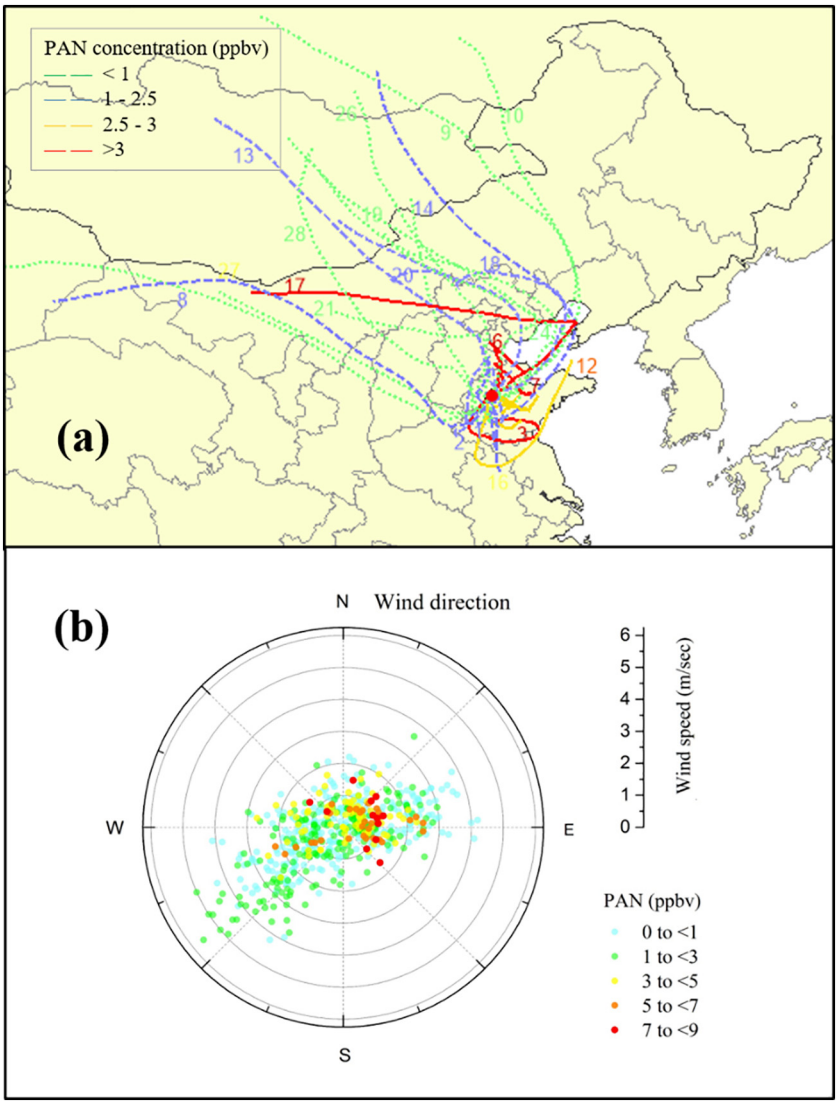

Fig. 4 – (a) The 72-hr back-trajectories for air masses 1000 m above sea level ending at 24:00 (16 UTC) in winter. Each of the 28 back trajectory lines, labeled 1–28, corresponded to one day consecutively from 18 Dec. 2015 to 14 Jan. 2016, (b) scatter diagram for PAN concentration level with respect to wind speed and direction during winter in Jinan. PAN: peroxyacetyl nitrate.

the rate constant for Reaction (R-2) (/sec); and k_3 is the rate constant for Reaction (R3) (cm^3/(molecule·sec)).

The equations above showed that the lifetime of PAN mainly depended on temperature and the ratio between the concentrations of NO_2 and NO. Considering the seasonal variation in temperature and high pollution levels (change of NO_2/NO) during haze episodes, we calculated the lifetime of PAN for three different situations: winter days without haze, winter days with haze, and summer days (Table 2). All rate constants were calculated by formulas recommended by National Institute of Standards and Technology (NIST) (Atkinson et al., 1997, 1992; Villalta and Howard, 1996). We chose the average value of the ratio between the concentrations of NO_2 and NO in every situation for the PAN lifetime calculation. Comparing the lifetime of PAN at three situations in Table 2, we determined that PAN lifetimes in winter with and without haze were 5.5 and 20 days, approximately 20 and 80 times longer than in summer (approximately 6 hr), respectively. The long lifetime of PAN in winter proved that the winter condition in Jinan favored the transport and accumulation of PAN. Compared with winter days without haze, the shorter lifetime of PAN during haze episodes because of lower [NO_2]/[NO] meant that the decomposition of PAN was much faster. The faster decomposition but higher levels of PAN during haze episodes combined with the discussion of case A in Section 2.2, implied that the photochemical generation of PAN might be faster than on common winter days. Furthermore, in contrast to PAN, the wintertime lifetime of ozone was mostly less than 1 hr (Zhang et al., 2014). Thus, except for intense O_3 titration of NO on the polluted days, the main reason of extremely low levels of O_3 during haze episodes was that O_3 was hard to be transported and accumulate like PAN.

2.4.2. Strong photochemical reactions during haze episodes

The generation rate of PAN was mainly affected by temperature, solar intensity and the concentrations of precursors, such

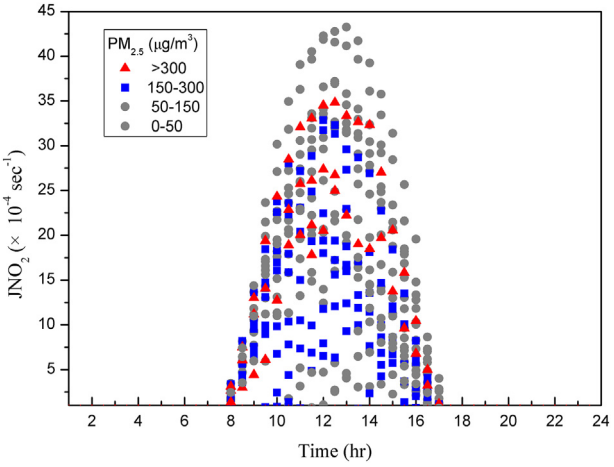

Fig. 5 – Diurnal variation in the photolysis rate constant of NO_2 ($J(NO_2)$) during winter color-coded by different concentrations of $PM_{2.5}$.

as VOCs and NO_x. As shown in Reaction (1) and Reaction (2), PAN was generated behind the formation of the peroxyacetyl (PA) radical which is derived from the OH-initiated oxidation or the photolysis of VOCs. The major VOC types for PA radical formation were concluded to be six carbonyls: acetaldehyde, acetone, methylglyoxal (MGLY), methacrolein (MACR), methyl vinyl ketone (MVK), and biacetyl (Altshuller, 1993; Cleary et al., 2007; Lafranchi et al., 2009), among which acetaldehyde was usually reported as the predominant source for PA radical production in urban areas (Kondo et al., 2008; Roberts et al., 2001). In addition, the PAN observation and model analysis at Beijing (2007) indicated that the major source (55%–75%) of PAN over China should be reactive aromatics (Liu et al., 2010), whose emissions and chemistry (major oxidation product, MGLY) had a significant impact on the understanding and assessment of photochemical pollution. The obvious drawback of our research was the deficiency of VOC monitoring, with which the analysis of PAN formation could be more reliable. Still, previous studies supported the notion that VOC concentrations obviously elevated during haze episodes (Liu et al., 2017; Sun et al., 2016; Wu et al., 2016), thus we roughly classified the high concentrations of VOCs into contributing factors of high-level PAN in winter.

In this study, light intensity during winter was illustrated by the photolysis rate constants of NO_2 ($J(NO_2)$), and the photolysis of NO_2 is mainly caused by the light at the 290–410 nm wavelengths (Atkinson et al., 2004). Fig. 5 shows the diurnal variation in $J(NO_2)$ during winter with respect to the $PM_{2.5}$ concentration. Although particles could clearly decrease the intensity of sunlight reaching the ground through scattering and absorption, in this study the high concentrations of particles did not show an obvious adverse effect on light intensity as expected. The inconspicuous negative correlation between photolysis rate constants of NO_2 and particle concentrations during haze might be related to the weather factors (such as clouds) and inhibiting effect on near-ultraviolet (UV) by diverse particle sizes, which was an interesting finding that deserved further investigation. Finally, we speculated that the solar radiations in photolysis band implied by moderate values

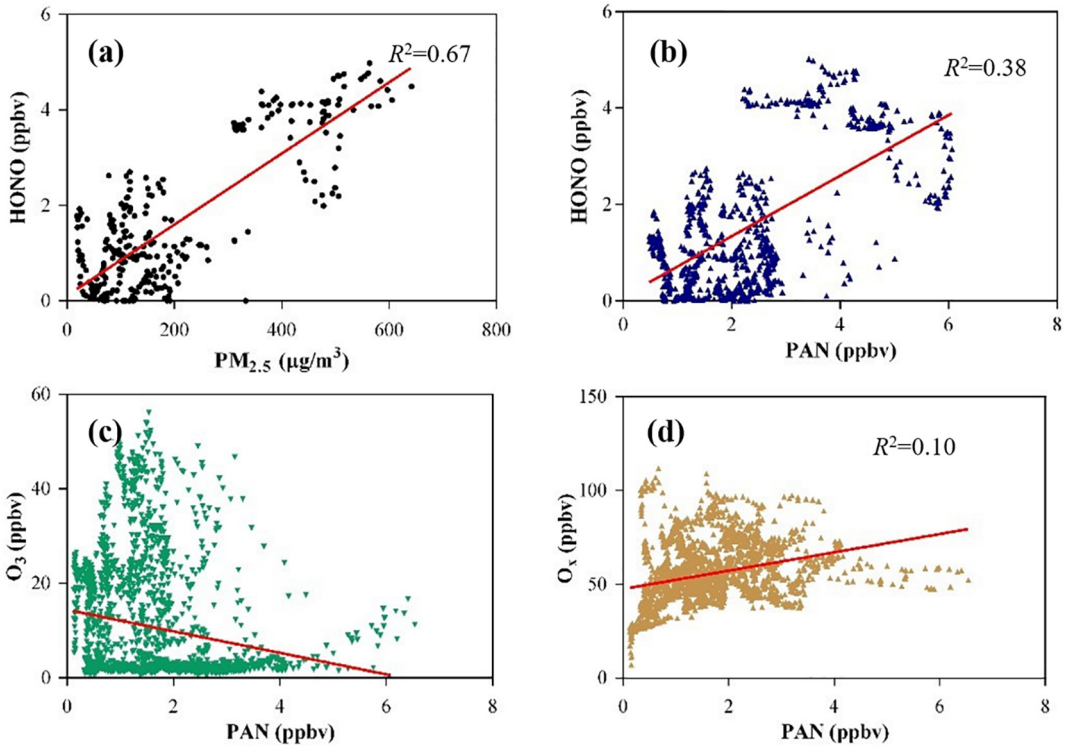

Fig. 6 – Scatter plots of HONO *vs.* $PM_{2.5}$ (a), HONO *vs.* PAN (b), O_3 *vs.* PAN (c), and O_x *vs.* PAN (d) at our site in winter. PAN: peroxyacetyl nitrate.

Table 2 – Comparison of PAN lifetimes and relevant reaction rate constants under different conditions.

Condition	k_2 ($\times 10^{-11}$) (cm^3/(molecule·sec))	k_{-2} ($\times 10^{-4}$) (/sec)	k_3 ($\times 10^{-11}$) (cm^3/(molecule·sec))	Temperature (K)	NO_2/NO	Lifetime (sec)
Typical winter day	1.29	0.137	2.16	275	39.42	1.79×10^6
Haze episodes	1.29	0.137	2.16	275	9.39	4.82×10^5
Summer day	1.19	8.20	1.99	300	26.30	2.20×10^4

k_2 refers to Atkinson et al., 1997, k_{-2} refers to Atkinson et al., 1992; k_3 refers to Villalta and Howard, 1996. PAN: peroxyacetyl nitrate.

of $J(NO_2)$ in severe haze episodes were enough to form strong photochemical reactions. This deduction was also supported by previous research on the efficiency of hydroxyl-radical-based self-cleansing (Rohrer et al., 2014), which proposed that in some urban situations the reactivity of OH radicals could be dominated by VOC or NO_x rather than by light intensity.

The main daytime source of OH radicals was normally the photolysis of O_3 in the presence of H_2O in clean air, but the photolysis of HONO was the predominant source of OH radicals in polluted atmosphere (especially in winter) (Lu et al., 2013). It was found that HONO contributed approximately 60% of the OH radicals during the daytime, followed by alkene ozonolysis (~24%), photolysis of HCHO (~16%) and O_3 (~5%) in Santiago, Chile (Elshorbany et al., 2009). The photolysis of HONO (<400 nm) could generate OH radicals, and the detailed formula is given in Reaction (4). The speculation that high PAN levels during haze episodes might be related to the enhancement of HONO concentration had been proposed in previous studies, but the concurrent data of HONO concentrations were lacking (Cheng et al., 2013; Tsang and Herron, 1991). In this study, we concurrently monitored HONO concentrations and other gas pollutants in winter to further verify our hypothesis.

$$HONO + h\upsilon \rightarrow HO + NO \quad (R4)$$

As shown in Fig. 6a, the positive correlation between HONO and $PM_{2.5}$ was clear with a linear correlation coefficient (R^2) of 0.67. There was an obvious enhancement of HONO concentration during haze episodes ($PM_{2.5}$ > 300 μg/m^3) and similar phenomenon was observed in previous studies (Cui et al., 2018; Hou et al., 2016). This enhancement of HONO might result from a higher heterogeneous conversion of NO_2 to HONO on the surface of abundant particles during haze episodes (Cui et al., 2018; Zhang and Mu, 2014). The mean value (3.70 ppbv) of HONO concentration during haze episodes in Jinan was much higher than that detected at Beijing (1.49 ppbv) (Hou et al., 2016), Guangzhou (2.80 ppbv) (Qin et al., 2009), and Santiago (1.44 ppbv) (Rubio et al., 2009). High levels of HONO during haze episodes could result in much more atmospheric OH radicals and would consequently contribute to the faster generation of PAN. The linear regression between the concentrations of HONO and PAN in winter with a linear correlation coefficient (R^2) of 0.38 also supported our hypothesis. Therefore, high levels of HONO could be a contributing factor for the rapid generation of PAN during haze episodes.

Although we well confirmed the deduction of strong photochemical reactions, the low levels of O_3 during haze episodes were still a contradiction. As shown in Fig. 6c, there was no positive correlation between PAN and O_3 in winter, which was found repeatedly in many studies (Kourtidis et al., 1993; Liu et al., 2010; Mcfadyen and Cape, 2005; Rappengluck et al., 1993). We had mentioned that O_3 was hard to accumulate and be transported like PAN due to its short lifetime, which could explain the poor correlation between PAN and O_3 in winter. The positive correlation between O_3 and wind velocity reported in previous study (Rappengluck et al., 1993) could confirm the above explanation. And the intense NO titration of O_3 in winter also contributed to that irrelevance, thus the linear regression between the concentrations of O_x (NO_2 + O_3) and PAN presented a better positive correlation. Finally, we concluded that the faster photochemical reactions during haze episodes and local accumulation were the main causes of the unusually high levels of PAN in winter. The high concentrations of precursors (NO_2, VOCs), the sufficient light intensity in the photolysis band and the high concentrations of HONO could well be the predominant reasons of faster (compared to common winter days) PAN photochemical production during haze episodes.

3. Conclusions

Peroxyacetyl nitrate concentrations, combined with the concurrent data of CCl_4, O_3, NO, NO_2, $PM_{2.5}$, HONO, photolysis rate constant of NO_2 and weather, were monitored continuously in Jinan, China from Nov. 2015 to Jul. 2016, which was the first detection of PAN in the urban area of Shandong Province. The result demonstrated that severe photochemical pollution occurred in Jinan during the study period, with maximum and mean values of PAN concentration: 9.6 and (1.89 ± 1.42) ppbv in winter, 13.5 and (2.54 ± 1.44) ppbv in summer, respectively. The main sources and formation mechanisms of PAN in winter were focused in the study due to the unusually high PAN concentrations. Backward trajectory analysis showed that only one night-time peak of PAN was associated with long-range transport, which suggested that air transport was a minor contributor to the unusually high PAN concentrations in winter, but local sources, such as photochemical reactions and accumulation, were major contributors. The lifetime of PAN in winter, as calculated by kinetics analysis and meteorological data, further supported our hypothesis that local PAN accumulation in winter contributes to high level PAN. In addition, the generation of PAN was expected to be faster on winter days with haze episodes than that on winter days without haze episodes, which deduced by the shorter lifetime but higher concentration of PAN during haze episodes. Finally, we concluded that the faster PAN generation during haze episodes might result from the high concentrations of precursors (NO_2 and VOCs), the sufficient light intensity in the photolysis band and the

high concentrations of HONO. This PAN research implied that severe photochemical pollution could also exist even in low-light conditions, such as haze, but the concurrently low levels of ozone were mostly due to short lifetime of ozone and the intense NO titration in polluted conditions. Simultaneous measurements of VOCs were recommended for future studies to increase the integrity of the experiment.

Severe photochemical pollution in the megacity of Jinan, China was reported in this study, and this information was useful to government agencies concerned with pollution control and management. Our study enriched the meager database of PAN research in China and provided model cases for further study of photochemical pollution. Furthermore, the results of this study might aid in understanding the complex chemical mechanisms of haze episodes, especially during winter.

Acknowledgments

This work was supported by the National Key R&D Program of China (No. 2016YFC0202700), the National Natural Science Foundation of China (Nos. 41375126, 21527814, 91743202), and the H2020 Marie Skłodowska-Curie Actions (No. H2020-MSCA-RISE-2015-690958).

REFERENCES

Aikin, A.C., Herman, J.R., Maier, E.J., Mcquillan, C.J., 1982. Atmospheric chemistry of ethane and ethylene. J. Geophys. Res. 87 (C4), 3105–3118.

Altshuller, A.P., 1993. Pans in the atmosphere. J. Air Waste Manage. Assoc. 43 (9), 1221–1230.

Atkinson, R., Baulch, D.L., Cox, R.A., Hampson, R.F., Kerr, J.A., Troe, J., 1992. Evaluated kinetic and photochemical data for atmospheric chemistry supplement — IV — IUPAC Subcommittee on Gas Kinetic Data Evaluation for Atmospheric Chemistry. J. Phys. Chem. Ref. Data 21 (6), 1125–1568.

Atkinson, R., Baulch, D.L., Cox, R.A., Hampson, R.F., Kerr, J.A., Rossi, M.J., et al., 1997. Evaluated kinetic, photochemical and heterogeneous data for atmospheric chemistry. 5. IUPAC Subcommittee on Gas Kinetic Data Evaluation for Atmospheric Chemistry. J. Phys. Chem. Ref. Data 26 (3), 521–1011.

Atkinson, R., Baulch, D.L., Cox, R.A., Crowley, J.N., Hampson, R.F., Hynes, R.G., Jenkin, M.E., Rossi, M.J., Troe, J., 2004. Evaluated kinetic and photochemical data for atmospheric chemistry: volume I — gas phase reactions of Ox, HOx, NOx and SOx species. Atmos. Chem. Phys. 4, 1461–1738.

Beine, H.J., Jaffe, D.A., Herring, J.A., Kelley, J.A., Krognes, T., Stordal, F., 1997. High-latitude springtime photochemistry. 1. NOx, PAN and ozone relationships. J. Atmos. Chem. 27 (2), 127–153.

Bottenheim, J.W., Gallant, A.J., 1989. Pan over the Arctic; observations during AGASP-2 in April 1986. J. Atmos. Chem. 9 (1–3), 301–316.

Cheng, P., Cheng, Y., Lu, K., Su, H., Yang, Q., Zou, Y., et al., 2013. An online monitoring system for atmospheric nitrous acid (HONO) based on stripping coil and ion chromatography. J. Environ. Sci. (China) 25 (5), 895–907.

Cleary, P.A., Wooldridge, P.J., Millet, D.B., McKay, M., Goldstein, A. H., Cohen, R.C., 2007. Observations of total peroxy nitrates and aldehydes: measurement interpretation and inference of OH radical concentrations. Atmos. Chem. Phys. 7 (8), 1947–1960.

Cui, L.L., Zhang, J., Zhang, J., Zhou, J.W., Zhang, Y., Li, T.T., 2016. Acute respiratory and cardiovascular health effects of an air pollution event, January 2013, Jinan, China. Public Health 131, 99–102.

Cui, L., Li, R., Zhang, Y., Meng, Y., Fu, H., Chen, J., 2018. An observational study of nitrous acid (HONO) in Shanghai, China: the aerosol impact on HONO formation during the haze episodes. Sci. Total Environ. 630, 1057–1070.

Elshorbany, Y.F., Kurtenbach, R., Wiesen, P., Lissi, E., Rubio, M., Villena, G., et al., 2009. Oxidation capacity of the city air of Santiago, Chile. Atmos. Chem. Phys. 9 (6), 2257–2273.

Fujiwara, H., Sadanaga, Y., Urata, J., Masui, Y., Bandow, H., Ikeda, K., et al., 2014. Aerial observation of nitrogen compounds over the East China Sea in 2009 and 2010. Atmos. Environ. 97 (SI), 462–470.

Gaffney, J.S., Marley, N.A., Prestbo, E.W., 1993. Measurements of peroxyacetyl nitrate at a remote site in the southwestern United-States — trophospheric implications. Environ. Sci. Technol. 27 (9), 1905–1910.

Gaffney, J.S., Marley, N.A., Cunningham, M.M., Doskey, P.V., 1999. Measurements of peroxyacyl nitrates (PANs) in Mexico City: implications for megacity air quality impacts on regional scales. Atmos. Environ. 33 (30), 5003–5012.

Gao, X., Yang, L., Cheng, S., Gao, R., Zhou, Y., Xue, L., et al., 2011. Semi-continuous measurement of water-soluble ions in PM2.5 in Jinan, China: temporal variations and source apportionments. Atmos. Environ. 45 (33), 6048–6056.

Grosjean, D., 1983. Distribution of atmospheric nitrogenous pollutants at a Los Angeles area smog receptor site. Environ. Sci. Technol. 17 (1), 13–19.

Grosjean, D., 2003. Ambient PAN and PPN in southern California from 1960 to the SCOS97-NARSTO. Atmos. Environ. 372, S221–S238.

Grosjean, E., Grosjean, D., Woodhouse, L.F., 2001. Peroxyacetyl nitrate and peroxypropionyl nitrate during SCOS97-NARSTO. Environ. Sci. Technol. 35 (20), 4007–4014.

Han, J., Lee, M., Lee, G., Emmons, L.K., 2017. Decoupling peroxyacetyl nitrate from ozone in Chinese outflows observed at Gosan Climate Observatory. Atmos. Chem. Phys. 17 (17), 1–29.

Hou, S.Q., Tong, S.R., Ge, M.F., An, J.L., 2016. Comparison of atmospheric nitrous acid during severe haze and clean periods in Beijing, China. Atmos. Environ. 124, 199–206.

Jacobi, H.W., Weller, R., Bluszcz, T., Schrems, O., 1999. Latitudinal distribution of peroxyacetyl nitrate (PAN) over the Atlantic Ocean. J. Geophys. Res. - Atmos. 104 (D21), 26901–26912.

Kean, A.J., Grosjean, E., Grosjean, D., Harley, R.A., 2001. On-road measurement of carbonyls in California light-duty vehicle emissions. Environ. Sci. Technol. 35 (21), 4198–4204.

Kenley, R.A., Hendry, D.G., 1982. Generation of peroxy-radicals from peroxynitrates ($ROONO_2$) — decomposition of peroxybenzoyl nitrate (PBZN). J. Am. Chem. Soc. 104 (1), 220–224.

Kondo, Y., Morino, Y., Fukuda, M., Kanaya, Y., Miyazaki, Y., Takegawa, N., et al., 2008. Formation and transport of oxidized reactive nitrogen, ozone, and secondary organic aerosol in Tokyo. J. Geophys. Res. - Atmos. 113 (1), 87–90.

Kourtidis, K.A., Fabian, P., Zerefos, C., Rappengluck, B., 1993. Peroxyacetyl nitrate (PAN), peroxypropionyl nitrate (PPN) and PAN ozone ratio measurements at 3 sites in Germany. Tellus Ser. B Chem. Phys. Meteorol. 45 (5), 442–457.

Lafranchi, B.W., Wolfe, G.M., Thornton, J.A., Browne, E.C., Min, K. E., Wooldridge, P.J., et al., 2009. Closing the peroxy acetyl (PA) radical budget: observations of acyl peroxy nitrates (PAN, PPN and MPAN) during BEARPEX 2009. Abstr. Pap. Am. Chem. Soc. 237, 289-289.

Lee, G., Jang, Y., Lee, H., Han, J.S., Kim, K.R., Lee, M., 2008. Characteristic behavior of peroxyacetyl nitrate (PAN) in Seoul megacity, Korea. Chemosphere 73 (4), 619–628.
Lee, J.B., Yoon, J.S., Jung, K., Eom, S.W., Chae, Y.Z., Cho, S.J., et al., 2013. Peroxyacetyl nitrate (PAN) in the urban atmosphere. Chemosphere 93 (9), 1796–1803.
Liu, Z., Wang, Y.H., Gu, D.S., Zhao, C., Huey, L.G., Stickel, R., et al., 2010. Evidence of reactive aromatics as a major source of peroxy acetyl nitrate over China. Environ. Sci. Technol. 44 (18), 7017–7022.
Liu, C., Ma, Z., Mu, Y., Liu, J., Zhang, C., Zhang, Y., et al., 2017. The levels, variation characteristics, and sources of atmospheric non-methane hydrocarbon compounds during wintertime in Beijing, China. Atmos. Chem. Phys. 17 (17), 10633–10649.
Lu, K.D., Hofzumahaus, A., Holland, F., Bohn, B., Brauers, T., Fuchs, H., et al., 2013. Missing OH source in a suburban environment near Beijing: observed and modelled OH and HO_2 concentrations in summer 2006. Atmos. Chem. Phys. 13 (2), 1057–1080.
Malley, C.S., Cape, J.N., Jones, M.R., Leeson, S.R., Coyle, M., Braban, C.F., et al., 2016. Regional and hemispheric influences on measured spring peroxyacetyl nitrate (PAN) mixing ratios at the Auchencorth UK EMEP supersite. Atmos. Res. 174, 135–141.
Marley, N.A., Gaffney, J.S., Ramos-Villegas, R., Gonzalez, B.C., 2007. Comparison of measurements of peroxyacyl nitrates and primary carbonaceous aerosol concentrations in Mexico City determined in 1997 and 2003. Atmos. Chem. Phys. 7 (9), 2277–2285.
Martini, F.M.S., Hasenkopf, C.A., Roberts, D.C., 2015. Statistical analysis of $PM_{2.5}$ observations from diplomatic facilities in China. Atmos. Environ. 110, 174–185.
McFadyen, G.G., Cape, J.N., 2005. Peroxyacetyl nitrate in eastern Scotland. Sci. Total Environ. 337 (1–3), 213–222.
Mellouki, A., Wallington, T.J., Chen, J., 2015. Atmospheric chemistry of oxygenated volatile organic compounds: impacts on air quality and climate. Chem. Rev. 115 (10), 3984–4014.
Mills, G.P., Sturges, W.T., Salmon, R.A., Bauguitte, S.J.B., Read, K.A., Bandy, B.J., 2007. Seasonal variation of peroxyacetylnitrate (PAN) in coastal Antarctica measured with a new instrument for the detection of sub-part per trillion mixing ratios of PAN. Atmos. Chem. Phys. 7 (17), 4589–4599.
Moore, D.P., Remedios, J.J., 2010. Seasonality of peroxyacetyl nitrate (PAN) in the upper troposphere and lower stratosphere using the MIPAS-E instrument. Atmos. Chem. Phys. 10 (13), 6117–6128.
Peak, M.J., Belser, W.L., 1969. Some effects of air pollutant, peroxyacetyl nitrate, upon deoxyribonucleic acid and upon nucleic acid bases. Atmos. Environ. 3 (4), 385–394.
Qin, M., Xie, P.H., Su, H., Gu, J.W., Peng, F.M., Li, S.W., et al., 2009. An observational study of the HONO–NO_2 coupling at an urban site in Guangzhou City, South China. Atmos. Environ. 43 (36), 5731–5742.
Rappengluck, B., Kourtidis, K., Fabian, P., 1993. Measurements of ozone and peroxyacetyl nitrate (PAN) in Munich. Atmos. Environ. B Urban Atmos. 27 (3), 293–305.
Roberts, J.M., Flocke, F., Weinheimer, A., Tanimoto, H., Jobson, B.J., Riemer, D., et al., 2001. Observations of APAN during TexAQS 2000. Geophys. Res. Lett. 28 (22), 4195–4198.
Roberts, J.M., Flocke, F., Stroud, C.A., Hereid, D., Williams, E., Fehsenfeld, F., et al., 2002. Ground-based measurements of peroxycarboxylic nitric anhydrides (PANs) during the 1999 Southern Oxidants Study Nashville Intensive. J. Geophys. Res. - Atmos. 107 (D21) (ACH-1-ACH 1–10).
Roberts, J.M., Jobson, B.T., Kuster, W., Goldan, P., Murphy, P., Williams, E., et al., 2003. An examination of the chemistry of peroxycarboxylic nitric anhydrides and related volatile organic compounds during Texas Air Quality Study 2000 using ground-based measurements. J. Geophys. Res. - Atmos. 108 (D16), 439–441.
Rohrer, F., Lu, K., Hofzumahaus, A., Bohn, B., Brauers, T., Chang, C.-C., et al., 2014. Maximum efficiency in the hydroxyl-radical-based self-cleansing of the troposphere. Nat. Geosci. 7 (8), 559–563.
Rubio, M.A., Lissi, E., Villena, G., Caroca, V., Gramsch, E., Ruiz, A., 2005. Estimation of hydroxyl and hydroperoxyl radicals concentrations in the urban atmosphere of Santiago. J. Chil. Chem. Soc. 50 (2), 471–476.
Rubio, M.A., Lissi, E., Villena, G., Elshorbany, Y.F., Kleffmann, J., Kurtenbach, R., et al., 2009. Simultaneous measurements of formaldehyde and nitrous acid in dews and gas phase in the atmosphere of Santiago, Chile. Atmos. Environ. 43 (38), 6106–6109.
Shao, M., Lu, S., Liu, Y., Xie, X., Chang, C., Huang, S., et al., 2009. Volatile organic compounds measured in summer in Beijing and their role in ground-level ozone formation. J. Geophys. Res. - Atmos. 114 (D2).
Stephens, E.R., Hanst, P.L., Doerr, R.C., Scott, W.E., 1956. Reactions of nitrogen dioxide and organic compounds in air. Ind. Eng. Chem. 48 (9), 1498–1504.
Sun, J., Wu, F., Hu, B., Tang, G., Zhang, J., Wang, Y., 2016. VOC characteristics, emissions and contributions to SOA formation during hazy episodes. Atmos. Environ. 141, 560–570.
Tsang, W., Herron, J.T., 1991. Chemical kinetic data-base for propellant combustion. 1. Reactions involving NO, NO_2, HNO, HNO_2, HCN and N_2O. J. Phys. Chem. Ref. Data 20 (4), 609–663.
Villalta, P.W., Howard, C.J., 1996. Direct kinetics study of the $CH_3C(O)O_2$ + NO reaction using chemical ionization mass spectrometry. J. Phys. Chem. 100 (32), 13624–13628.
Wang, T., Poon, C.N., Kwok, Y.H., Li, Y.S., 2003. Characterizing the temporal variability and emission patterns of pollution plumes in the Pearl River Delta of China. Atmos. Environ. 37 (25), 3539–3550.
Wang, B., Shao, M., Roberts, J.M., Yang, G., Yang, F., Hu, M., et al., 2010. Ground-based on-line measurements of peroxyacetyl nitrate (PAN) and peroxypropionyl nitrate (PPN) in the Pearl River Delta, China. Int. J. Environ. Anal. Chem. 90 (7), 548–559.
Wang, X., Wang, W., Yang, L., Gao, X., Nie, W., Yu, Y., et al., 2012. The secondary formation of inorganic aerosols in the droplet mode through heterogeneous aqueous reactions under haze conditions. Atmos. Environ. 63, 68–76.
Wen, L., Chen, J., Yang, L., Wang, X., Wang, W., Xu, C., et al., 2015. Enhanced formation of fine particulate nitrate at a rural site on the North China Plain in summer: the important roles of ammonia and ozone. Atmos. Environ. 101, 294–302.
Whalley, L.K., Lewis, A.C., Mcquaid, J.B., Purvis, R.M., Lee, J.D., Stemmler, K., et al., 2004. Two high-speed, portable GC systems designed for the measurement of non-methane hydrocarbons and PAN: results from the Jungfraujoch High Altitude Observatory. J. Environ. Monit. 6 (3), 234–241.
Wolfe, G.M., Thornton, J.A., Mcneill, V.F., Jaffe, D.A., Reidmiller, D., Chand, D., et al., 2007. Influence of trans-Pacific pollution transport on acyl peroxy nitrate abundances and speciation at Mount Bachelor Observatory during INTEX-B. Atmos. Chem. Phys. 7 (20), 5309–5325.
Wu, R., Li, J., Hao, Y., Li, Y., Zeng, L., Xie, S., 2016. Evolution process and sources of ambient volatile organic compounds during a severe haze event in Beijing, China. Sci. Total Environ. 560, 62–72.
Xu, J., Zhang, Y., Fu, J.S., Zheng, S., Wang, W., 2008. Process analysis of typical summertime ozone episodes over the Beijing area. Sci. Total Environ. 399 (1–3), 147–157.
Xu, Z., Wang, T., Wu, J., Xue, L., Chan, J., Zha, Q., et al., 2015. Nitrous acid (HONO) in a polluted subtropical atmosphere: seasonal variability, direct vehicle emissions and heterogeneous production at ground surface. Atmos. Environ. 106, 100–109.
Yang, L.X., Wang, D.C., Cheng, S.H., Wang, Z., Zhou, Y., Zhou, X.H., et al., 2007. Influence of meteorological conditions and particulate matter on visual range impairment in Jinan, China. Sci. Total Environ. 383 (1–3), 164–173.
Yang, L., Zhou, X., Wang, Z., Zhou, Y., Cheng, S., Xu, P., et al., 2012. Airborne fine particulate pollution in Jinan, China: concentrations,

chemical compositions and influence on visibility impairment. Atmos. Environ. 55, 506–514.
Zhang, G., Mu, Y., 2014. Seasonal and diurnal variations of atmospheric peroxyacetyl nitrate, peroxypropionyl nitrate, and carbon tetrachloride in Beijing. J. Environ. Sci. 26 (1), 65–74.
Zhang, J.M., Wang, T., Ding, A.J., Zhou, X.H., Xue, L.K., Poon, C.N., et al., 2009. Continuous measurement of peroxyacetyl nitrate (PAN) in suburban and remote areas of western China. Atmos. Environ. 43 (2), 228–237.
Zhang, J.B., Xu, Z., Yang, G., Wang, B., 2011. Peroxyacetyl nitrate (PAN) and peroxypropionyl nitrate (PPN) in urban and suburban atmospheres of Beijing, China. Atmos. Chem. Phys. Discuss. 11 (3), 8173–8206.
Zhang, G., Mu, Y., Liu, J., Mellouki, A., 2012. Direct and simultaneous determination of trace-level carbon tetrachloride, peroxyacetyl nitrate, and peroxypropionyl nitrate using gas chromatography–electron capture detection. J. Chromatogr. A 1266 (1), 110–115.
Zhang, H., Xu, X., Lin, W., Wang, Y., 2014. Wintertime peroxyacetyl nitrate (PAN) in the megacity Beijing: role of photochemical and meteorological processes. J. Environ. Sci. 26 (1SI), 83–96.
Zhang, G., Mu, Y., Zhou, L., Zhang, C., Zhang, Y., Liu, J., et al., 2015. Summertime distributions of peroxyacetyl nitrate (PAN) and peroxypropionyl nitrate (PPN) in Beijing: understanding the sources and major sink of PAN. Atmos. Environ. 103, 289–296.